

A DC Optimal Power Flow Approach to Quantify Operational Resilience in Power Grids



Zarif Ahmet Zaman and Edoardo Patelli

Abstract The primary objective of resilience engineering is to analyse and mitigate the risk of a system once a vulnerability has been triggered by an attack. Resilience is a multidimensional concept in the field of engineering and incorporates restoration in the form of a performance and time. Nodal restoration is a key factor in the analysis of resilience in systems, and the properties of the nodes can be analysed to assess the states on the system. The model proposed for the power grid to demonstrate the failure of the network has been used to simulate probability of contingencies on the system and applies a Sequential Monte Carlo simulation to simulate the energy supplied. Additionally, a weather model incorporating the effects of both severe winds and lightning storms has been applied to act as a trigger to the contingency. Once failure of one component has occurred, it cannot be repaired until the network's performance reaches zero. Given failure of all components, the network will immediately start its restoration phase, and using the same algorithm for optimal power flow calculations, a DC power flow approach is implemented to assess the energy supplied to the whole network in a transient model until the network's loads meet the demand criteria completely.

Keywords Power-grid · Risk · Resilience · DC-OPF · Uncertainty

1 Introduction

The power grid is an essential tool for modern society and its function is crucial for the wellbeing of people. A failure of the system can lead to major consequences, in a socio-economic scale. The assessment of reliability in power grid systems and the parameters incorporating reliability in the power grid such as availability, consequence modelling and energy not supplied has been an important field of research

Z. A. Zaman

Institute for Risk and Uncertainty, University of Liverpool, Liverpool, UK

E. Patelli (✉)

Department of Civil and Environmental Engineering, University of Strathclyde, Glasgow, UK

e-mail: edoardo.patelli@strath.ac.uk

for the IEEE community. Past events such as the 2003 British National Power Grid Corporation outage which was responsible for the load loss of 724 MW, or approximately 20% of London's power load have costed the UK a significant economic burden [1].

The reliability of any system can be defined as the probability of success of the system at a given period of time, and the knowledge of reliability plays a role for system engineering to enable system maintenance planning to optimize risk mitigation [2]. System reliability can be thought of as a multidimensional analysis and incorporates many parameters. The user can analyse a single metric or multiple metrics simultaneously. The constraint with complex systems is developing the most computationally inexpensive technique and producing the most accurate results, with the aim to maximise the efficiency of the simulation.

Rochetta et al. developed a load flow approach to calculate failure probabilities from contingencies incorporating a wind model [3]. This was further developed with an artificial neural network surrogate model to act as a meta model for the analysis in order to minimise computational time when applied to AC optimal power flow calculations [4]. This model was developed on the basis of a severe weather model which was developed by Cadrini et al. [5] which combines stochastic extreme weather model and realistic power grid fault dynamics in order to model a restoration model quantified by sequential Monte Carlo. The constraint placed when applying this model is the high computational cost for the resilience function, especially when assessing networks with large scales of nodes.

There are various definitions of resilience available, both in a scientific context and a general context. The United Nations International Strategy for Disaster Reduction defines resilience as "The capacity of a system, community or society potentially exposed to hazards to adapt, by resisting or changing to reach and maintain an acceptable level of functioning and structure" [6]. However in a more specific context from that of extreme weather events, the definition of resilience can be thought of as "the network ability to withstand high impact low probability events, rapidly recovering and improving operations and structures to mitigate the impact of similar events in the future" [7]. Efforts placed on quantification of resilience analysis have been limited and have only been tested in the last 20 years. Additionally, such efforts placed into resilience analysis applied to the power grid have been performed, which includes various techniques such as transient performance modelling for the case study of typhoon Bolaven in South Korea [8]. However the authors mentioned that the limitations in their study included only computing resilience in the form of restorative and absorptive capacity without considering anticipated and adaptive capacities and also did not include a cost benefit analysis for the quantification of resilience in an economic sense. Panteli et al. developed a method to quantify resilience in the power function n with extreme weather events by developing the three phase resilience trapezoid [9]. This is an extension to the traditional resilience triangle developed in prior literature [10] which involves three stages to the disintegration, stagnation and recovery of the structure. The author divides resilience into two types, infrastructural and operational, stating that infrastructural resilience is in a more vulnerable condition given its recovery times and damage done to the system. Kim et. al developed

a novel function to analyse the South Korean power grid network using cascading failure analysis using three different node centrality metrics; degree, clustering coefficient and betweenness [11]. A high clustering coefficient of a network indicates a more resilient network as it contains a higher redundancy potential as alternative paths in the network's nodes are present. Resilience has also been portrayed in the field of structural engineering [12] by associating a structural resilience index to for both a pre-event and post-event state. The arbitrary structural resilience index is conformed from certain parameters deduced by the nature of the structure as stated in the article.

1.1 Proposed Approach

This paper aims to apply a DC optimal power flow approach to quantify resilience in a simple power grid system after a network failure has occurred. The novel theme of this paper is the application of resilience as an extension to the weather induced model introduced in [3]. The chosen application for modelling will be MATLAB 2020b and the application will be case 9 as obtained from MATPower.

2 Resilience Model

The index of resilience chosen for the power grid system is the Expectation of Energy Not Supplied which is deemed to be the most appropriate performance and has historically been used as an indicator of reliability performance and can further be extended for resilience analysis. The equation listed below states the resilience index as a dividend of the load received and the expected load:

$$ENS = \sum_{t=1}^{T_{sim}} \sum_{i \in N} L_{cut,i,t} \cdot t \quad (1)$$

where T_{sim} is the simulation time and $L_{cut,i,t}$ is the load curtailed at each individual node during time t .

2.1 Optimization

In the case of optimization, the two models are the DC Optimal Power Flow approach and the AC Optimal Power Flow approach. In the real life power grid system, the electricity is generated in power plants using methods such as fossil fuels, converted fuels or geothermal steam and transfer this energy through the transmission network at high

voltage using either DC or AC flow [13]. This high voltage steps down into a medium voltage range. The primary difference between the DC and AC optimal power flow models is the convexity. DC power is constantly in a steady state, and therefore is both a linear and convex optimization problem. However, AC optimal power flow calculations are non-linear and non-convex leading to much higher computational expense. It should also be noted that in high-fidelity models, DC optimal power flow are limited in terms of details for these grids as noted by [14]. This is due to DC optimal power flow models being an estimation of AC optimal power flow models and only accounts for active power, without reactive power in the model [15]. The equations for optimal power flow approach can be denoted below as obtained from [16]. The standard optimization vector is defined as:

$$\min_x f(x) \quad (2)$$

Subject to

$$g(x) = 0 \quad (3)$$

$$h(x) \leq 0 \quad (4)$$

$$x_{min} \leq x \leq x_{max} \quad (5)$$

The optimization vector for DC optimal power flow neglects reactive power and voltage magnitude and is defined as;

$$x = \begin{bmatrix} \theta \\ P_g \end{bmatrix} \quad (6)$$

Equation 2 is reduced to;

$$\min_{\theta, P_g} \sum_{i=1}^{n_g} f_p^i(p_g^i) \quad (7)$$

2.2 Load Contingencies

The representation of failure for this model will be in the form of contingencies. In this context, a contingency is defined as an event occurring that is not considered predictable at a given time. Contingencies when applied to the power grid network imply the network's architecture is the disruption of the load transfer from one bus

to the next. This is commonly caused by a failure by extremely hot weather, system failure such as outages in loads and human errors [17].

2.3 Severe Weather Model

In extension to the contingencies faced in the model, a weather model has been proposed in the simulation algorithm to mimic the real-life application of an event. These events include lightning strikes, extremely high winds and natural disasters. The occurrence of normal weather conditions can be modelled as a homogeneous Poisson process. All equations for this weather model have been taken from [18].

$$P(N_f(t) = k) = \frac{[\lambda_n \cdot t]^k}{k!} e^{-\lambda_n \cdot t} \quad k = 0, 1, \dots, N \quad (8)$$

Where $P(N_f(t) = k)$ represents the probability that k failures happen within the network given the time $(0, t)$ and $N_f(t)$ is the number of failures per kilometre of grid line. However, in a more realistic perspective, the weather model is more likely to be affected by uncertainty. Therefore the occurrence of severe weather events is more suited to be modelled by a Non-homogeneous Poisson process:

$$P(N_f(t) = k) = \frac{[\lambda_n \cdot t]^k}{k!} e^{-\lambda_n \cdot t} \quad k = 0, 1, \dots, N \quad (9)$$

In this case, $V_e(t)$ represents the time dependent probability of the event occurring and can be obtained applying the following equation:

$$V_e(t) = \int_t^0 v_e(t') dt' \quad (10)$$

$v_e(t')$ is the rate at which the disturbance occurs. Given a severe weather occurrence in a storm consisting of severe winds and lightning strikes, the time of the event is obtained from data from previous events and will be carried out using probability distribution functions obtained from the variables listed in Table 1.

In the case of high winds, the windstorm intensity is obtained via the following equations:

$$W_\omega(t) = W_{crt} + \Delta_\omega(t) \quad (11)$$

where $W_w(t)$ is the wind speed intensity at time t for the and W_{crt} is a datum wind speed known as the critical wind speed set at 10 m/s. $\Delta_w(t)$ is the difference between the critical wind speed and the actual wind speed during the event. In terms of the lightning severe weather model, the intensity of a the weather event is set at the

Table 1 Variable attributes

	Distribution	Scale (a)	Shape (b)
$D\omega$	Weibull	9.86	1.17
D_{lg}	Weibull	0.96	0.85
$\Delta_{\omega}(t)$	Weibull	1.23	1.05
		Mean (μ_{Ng})	SD (σ_{Ng})
$N_g(t)$	Log-normal	-5.34	1.07

lightning strike ground density $N_g(t)$ which takes the units of ground flashes per unit time and area [occh km^2] modelled with log-normal variability.

The table below shows the shape and scale factors for the respective variables:

Both high winds and lightning strikes are a cause of contingency and therefore it is crucial to define an equation which considers both contingencies to calculate the total failure rate:

$$\lambda(t) = \lambda_n + \lambda_{\omega}(W_{\omega}(t)) + \lambda_{lg}(N_g(t)) \tag{12}$$

λ_w is the total line failure contribution due to high wind measured per km and $\lambda_{(lg)}$ is the lightning storms contribution. When considering individual lines, the contribution to line failure due to high winds can be denoted in the equation;

$$\lambda_{\omega}(W_{\omega}(t)) = \lambda_n \left(\frac{W_{\omega}(t)^2}{W_{crt}^2} - 1 \right) \alpha_{\omega} \tag{13}$$

α_w is the regression parameter for failure data obtained from the literature. The line failure rate as a result of lightning can be denoted as:

$$\lambda_{lg}(N_g(t)) = \lambda_n \beta_{lg} N_g(t) \tag{14}$$

β_{lg} is the regression coefficient obtained from prior data [18].

2.4 Repair Speed

The model for recovery has been obtained from [5] and takes into consideration the efficiency of the repair crew as they are also affected by the adverse weather conditions. The assumptions in this model are:

- i. Repair is initiated instantly after failure
- ii. After a line is repaired, it is considered fully functional
- iii. The transitional time between failure and repair is negligible.

$$v_{repair} = \begin{cases} \frac{v_{norm}}{1+\eta \cdot (W_{\omega}(t) - W_{crt})}, & \text{if } W_{\omega}(t) \geq W_{crt}, N_g = 0 \\ \frac{v_{norm}}{1+\Psi \cdot N_g}, & \text{if } W_{\omega}(t) < W_{crt}, N_g > 0 \\ \frac{v_{norm}}{[1+\eta \cdot (W_{\omega}(t) - W_{crt})] + [1+\Psi \cdot N_g]}, & \text{if } W_{\omega}(t) \geq W_{crt}, N_g > 0 \end{cases}$$

In this model and η are positive parameters and v_{norm} is set at 20[%/h]. The values for Ψ and η are set to 40 and 0.4, respectively.

2.5 Probabilistic Load Uncertainty

It is important to quantify uncertainty in the model used which uses data for variability in average daily load demand. The aleatory uncertainty of the model can be considered by implementing a gaussian with parameters fitted on historical data;

$$f(L_i(t)) = \frac{1}{\sqrt{2\pi}\sigma_{L_i}(t)} e^{-\frac{L_i(t) - \mu_{L_i}(t)}{2\sigma_{L_i}(t)^2}} \quad (15)$$

The parameters implemented are $L_i(t)$ is the transient node demand at node i during a specific hour of the day denoted as t . $\mu_{L_i}(t)$ is the mean load value and $\sigma_{L_i}(t)$ is the standard deviation of node i at time t . The gaussian will be applied at each output value with the standard deviation obtained from the equation subject to the variance from the parameters listed. An assumption of this model is that seasonal effects do not play a role in the parameter values.

3 Methodology

The proposed approach applied is a DC optimal power flow approach to quantify the energy not supplied during the severe weather contingency, which has been applied to quantify the resilience function of energy supplied after disaster through the same algorithm. The implementation of the methodology is applied using MATLAB 2020b, and the inputs are the parameters listed in Table 1. The network is presented with failure from a single contingency simulated from the risk model combining high winds and lightning strikes from Eqs. 10–14 and is implemented on the power flow equations to calculate the loss of load for disaster, and following this, the energy supplied after the disaster has occurred. The simulation is repeated until the network's performance has been fully restored. The pseudocode below displays the steps of the proposed approach below;

Algorithm 1 DC Optimal Power Flow model

```

1: procedure ENS (Risk Assessment based on DC-OPF)
2:   Input =  $\{\lambda_n, \beta_{lg}, \alpha_w, W_{crit}, b_{Dw}, a_{Dlg}, b_{Dlg}, a_{\Delta w}, b_{\Delta w}, v_{norm}, \mu_{Ng}, \sigma_{Ng}\}$ 
3:    $t = 0, e = 1, f = 0$ 
4:   Sample failure events for  $[0, T_{sim}]$ 
5:    $t = TTE(e)$ 
6:   if event i is a failure then
7:      $f = f + 1$ 
8:     Sample  $X_f$  and  $L_f$  for  $t$ 
9:     Update repair speed and time to repair
10:    else Sample  $Te$  and  $(N_g, \Delta_w)$ 
11:     Compute failure rates
12:     if  $t + TTF(f) > t + T_d$  then
13:       Compute load
14:       Compute ENS(f) using  $L_{cut}(f)$  and  $TTR(f)$ 
15:     else set  $t = t + T_d$  and  $f = f + 1$ 
16:   Sample  $X_f$  and  $L_f$  for  $t$ 
17:   Update repair speed and time to repair
18:   OUTPUT - Energy Not Supplied

```

4 Case Study

This paper implements case 9 as an example from MATPower's default folders [19]. It is composed of a 9-node, 9-line network which is assumed to be equidistant in all lines. This file was chosen due to the ring style topology which represents a simplified version of a small landlocked country in nature (Fig. 1).

The power grid's network lines represent the various branches with a 10-mile length. The failure rates of each branch have been obtained from the original MATPower file and have been implemented in the table. The failure rate is given as a relative probability of a line contingency for each individual line (Table 2).

4.1 Results

The recovery time initiates after 1×10^{-4} s in the simulation and continues to restore the energy supplied to the nodes are fully recovered after 4×10^{-4} s, in which the system has fully recovered and therefore all the energy required for the nodes in the whole network is being supplied. The uncertainty applied from Eq. 15 shows the

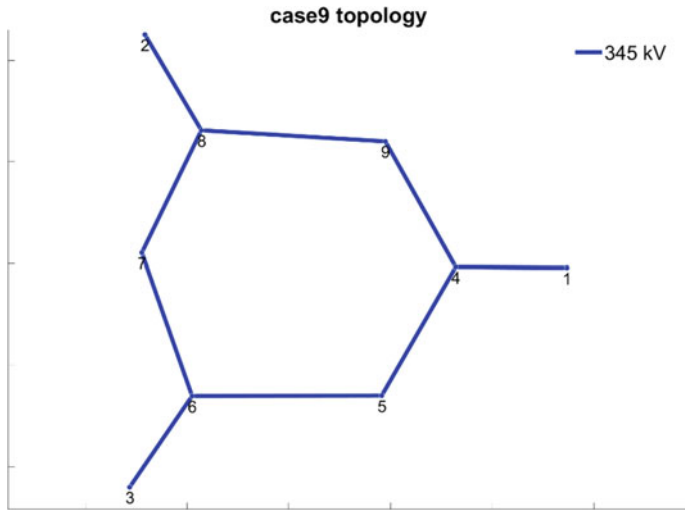


Fig. 1 Topology of case 9 network under matter to remain

Table 2 Branch failure rates [19]

Branch	Relative failure rate
1-4	0.1455
4-5	0.8693
5-6	0.5797
3-6	0.5499
6-7	0.1450
7-8	0.8530
8-2	0.6221
8-9	0.3510
9-4	0.5132

possible ranges of the energy supplied to the recovery function which also converges in the latter stages of the simulation. The model restores energy to each individual node simultaneously and therefore the restoration of all nodes improves rapidly during initial recovery, however, requires a start-up time in which no nodes are recovering. This initial period lasts less than 1 s of the simulation time and then increases rapidly. The drive for a lower range of uncertainty can be trialled by using more Monte Carlo simulations which are likely to sample more simulations on the same target output, energy not supplied leading to lower variance in results in output energies (Fig. 2).

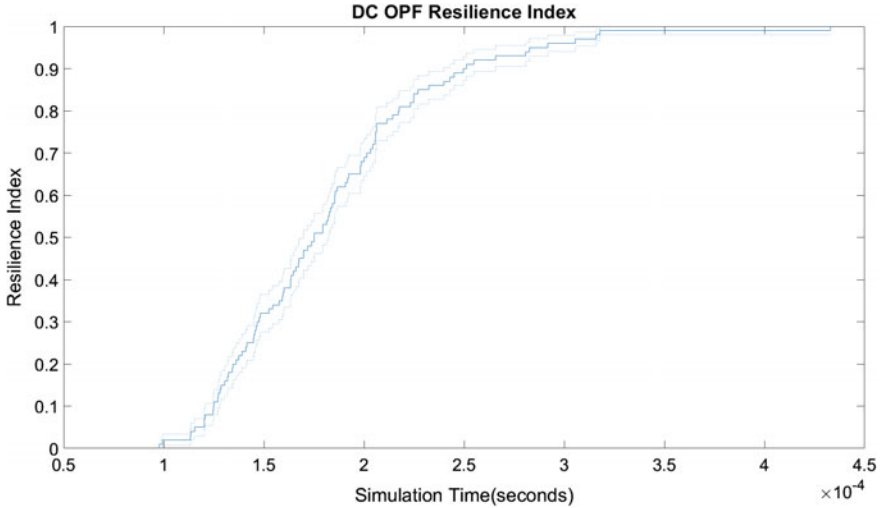


Fig. 2 Results for DC-OPF simulation under matter to remain

5 Conclusion

This paper demonstrates the application of a restoration function applied to a simple power network when DC optimal power flow is applied to the 9-node example provided in MATPower by applying a Monte Carlo approach. The work presented has innovated the weather model applied to contingencies in the general power grid to the application of resilience for the energy supplied after disaster. Further work that could be done on this topic includes developing a cost model for resilience quantification for the respective nodes in the network, and further expanding this application into three phase resilience models for realistic and complex networks using real time event timelines, rather than timelines based on simulation only.

References

1. Shuai, M., Chengzhi, W., Shiwen, Y., Hao, G., Jufang, Y., & Hui, H. (2018). Review on economic loss assessment of power outages. *Procedia Computer Science*, 130, 1158–1163. The 9th International Conference on Ambient Systems, Networks and Technologies (ANT 2018)/The 8th International Conference on Sustainable Energy Information Technology (SEIT-2018).
2. Koker, N. D., Viljoen, C., Lenner, R., & Jacobsz, S. (2020). Updating structural reliability efficiently using load measurement. *Structural Safety*, 84.
3. Rocchetta, R., Zio, E., & Patelli, E. (2018). A power-flow emulator approach for re-silience assessment of repairable power grids subject to weather-induced failures and data deficiency. *Applied Energy*, 210, 339–350. <https://doi.org/10.1016/j.apenergy.2017.10.126.6>.

4. Rocchetta, R., Bellani, L., Compare, M., Zio, E., & Patelli, E. (2019). A reinforcement learning framework for optimal operation and maintenance of power grids. *Applied Energy*, 241, 291–301. <https://doi.org/10.1016/j.apenergy.2019.03.027>.
5. Cadini, G. L., Agliardi, E., & Zio. (2017). A modeling and simulation framework for the reliability/availability assessment of a power transmission grid subject to cascading failures under extreme weather conditions. *Applied Energy*, 185, 267–279. <https://doi.org/10.1016/j.apenergy.2016.10.086>
6. I.P. on Climate Change, Climate Change. (2013). The Physical Science Basis: Working Group I Contribution to the Fifth Assessment Report of the Intergovernmental Panel on Climate Change, Cambridge University Press.
7. Panteli, M., & Mancarella, P. (2015). Influence of extreme weather and climate change on the resilience of power systems: Impacts and possible mitigation strategies. *Electric Power Systems Research*, 27, 259–270. <https://doi.org/10.1016/j.epr.2015.06.012>.
8. Jufri, F. H., Widiputra, V., & Jung, J. (2019). State-of-the-art review on power grid resilience to extreme weather events: Definitions, frameworks, quantitative assessment methodologies, and enhancement strategies. *Applied Energy*, 239, 1049–1065. <https://doi.org/10.1016/j.apenergy.2019.02.017>
9. Panteli, M., Mancarella, P., Trakas, D. N., Kyriakides, E., & Hatziazi-gyriou, N. D. (2017). Metrics and quantification of operational and infrastructure resilience in power systems. *IEEE Transactions on Power Systems*, 32(6), 4732–4742. <https://doi.org/10.1109/TPWRS.2017.2664141>.
10. Bruneau, M., Chang, S. E., Eguchi, R. T., Lee, G. C., O'Rourke, T. D., Reinhorn, A. M., et al. (2003). A framework to quantitatively assess and enhance the seismic resilience of communities. *Earthquake Spectra*, 19(4), 733–752. <https://doi.org/10.1193/1.1623497>.
11. Kim, D. H., Eisenberg, D. A., Chun, Y. H., & Park, J. (2017). Network topology and resilience analysis of South Korean power grid. *Physica A: Statistical Mechanics and its Applications*, 465, 13–24. <https://doi.org/10.1016/j.physa.2016.08.002>
12. Chiaia, B., Barchiesi, E., Biagi, V. D., & Placidi, L. (2019). A novel structural resilience index: Definition and applications to frame structures. *Mechanics Research Communications*, 99, 52–57. <https://doi.org/10.1016/j.mechrescom.2019.03.007>.
13. Amini, M. H., Bahrami, S., Kamyab, F., Mishra, S., Jaddivada, R., Boroo-jeni, K., Weng, P., & Xu, Y. (2018). Chapter 6—Decomposition methods for distributed optimal power flow: Panorama and case studies of the dc model. In: A. F. Zobaa, S. H. A. Aleem, & A. Y. Abdelaziz (Eds.), *Classical and recent aspects of power system optimization* (pp. 137–155). Academic Press. <https://doi.org/10.1016/B978-0-12-812441-3.00006-9>
14. Li, J., Tan, G., Cheng, B., Liu, D., & Pan, W. (2017). Transport mechanism of chitosan-n-acetylcysteine, chitosan oligosaccharides or carboxymethyl chitosan decorated coumarin-6 loaded nanostructured lipid carriers across the rabbit ocular. *European Journal of Pharmaceutics and Biopharmaceutics*, 120, 89–97. <https://doi.org/10.1016/j.ejpb.2017.08.013>.
15. Hertem, D. V.: Usefulness of dc power flow for active power flow analysis with flow controlling devices. In: *IET Conference Proceedings* (pp. 58–62(4)).
16. Li, J., Shi, C., Chen, C., & Duenas-Osorio, L. (2018). A cascading failure model based on ac optimal power flow: Case study. *Physica A: Statistical Mechanics and its Applications*, 508, 313–323. <https://doi.org/10.1016/j.physa.2018.05.081>.
17. Golari, M., Fan, N., & Wang, J. (2014). Two-stage stochastic optimal islanding operations under severe multiple contingencies in power grids. *Electric Power Systems Research*, 114, 68–77. <https://doi.org/10.1016/j.epr.2014.04.007>.
18. Alvehag, K., & Soder, L. (2011). A reliability model for distribution systems incorporating seasonal variations in severe weather. *IEEE Transactions on Power Delivery*, 26(2), 910–919. <https://doi.org/10.1109/TPWRD.2010.2090363>.
19. Zimmerman, R. D., Murillo-Sánchez, C. E., & Thomas, R. J. (2011). Matpower: Steady-state operations, planning, and analysis tools for power systems research and education. *IEEE Transactions on Power Systems*, 26(1), 12–19.